Overpressurized bubbles versus voids formed in helium implanted and annealed silicon

P. F. P. Fichtner, J. R. Kaschny, R. A. Yankov, A. Mücklich, U. Kreißig, and W. Skorupa

Citation: Applied Physics Letters **70**, 732 (1997); doi: 10.1063/1.118251
View online: http://dx.doi.org/10.1063/1.118251
View Table of Contents: http://scitation.aip.org/content/aip/journal/apl/70/6?ver=pdfcov
Published by the AIP Publishing

Overpressurized bubbles versus voids formed in helium implanted and annealed silicon

P. F. P. Fichtner,[a] J. R. Kaschny, R. A. Yankov, A. Mücklich, U. Kreißig, and W. Skorupa
Institute of Ion Beam Physics and Materials Research, Research Center Rossendorf, Inc., POB 510119, D-01314 Dresden, Germany

(Received 27 September 1996; accepted for publication 2 December 1996)

The formation of helium induced cavities in silicon is studied as a function of implant energy (10 and 40 keV) and dose (1×10^{15}, 1×10^{16}, and 5×10^{16} cm^{-2}). Specimens are analyzed after annealing (800 °C, 10 min) by transmission electron microscopy (TEM) and elastic recoil detection (ERD). Cavity nucleation and growth phenomena are discussed in terms of three different regimes depending on the implanted He content. For the low (1×10^{15} cm^{-2}) and high (5×10^{16} cm^{-2}) doses our results are consistent with the information in the literature. However, at the medium dose (1×10^{16} cm^{-2}), contrary to the gas release calculations which predict the formation of empty cavities, ERD analysis shows that a measurable fraction of the implanted He is still present in the annealed samples. In this case TEM analyses reveal that the cavities are surrounded by a strong strain field contrast and dislocation loops are generated. The results obtained are discussed on the basis of an alternative nucleation and growth behavior that allows the formation of bubbles in an overpressurized state irrespective of the competition with the gas release process. © *1997 American Institute of Physics.* [S0003-6951(97)01306-5]

Helium is usually incorporated in solids as a result of nuclear or ion beam related processes. Due to its extremely low solubility, He segregates into small gas-vacancy complexes, thus favoring the formation of bubbles (i.e., gas filled cavities) which inevitably coarsen upon high temperature annealing. As opposed to the case of metals, the He gas in silicon can be released from the bubbles, permeate through the matrix, and evaporate from the surface at temperatures much lower than the Si melting point. In effect, depending on both the anneal parameters and gas concentration, one is left with a system of voids (i.e., gas empty cavities). This behavior has been first studied by Griffioen *et al.*[1] in Si implanted at high He doses and low energies (typically 2×10^{17} cm^{-2} and 10 keV).

More recently, Myers *et al.*[2] have demonstrated that He induced cavities are very efficient in trapping metal impurities such as Cu and Au. Their work has stimulated further exploration in this field with the aim of developing proximity gettering techniques for very large scale integration (VLSI) applications.[3–5] Most of these studies have concentrated on high dose implants producing a high number density of cavities. For VLSI devices, however, not only very low impurity levels,[3] but also low defect densities are required. This implies that, from the viewpoint of device processing optimization, it would be desirable to reduce the He dose necessary to create a local gettering void system.

In the present letter we report experimental results shedding new light on the He induced cavity phenomena in Si. The emphasis of our study is placed on Si implanted with relatively low He doses where, after annealing, a rather low number density of cavities is formed. Such structures are further referred to as diluted cavity systems in order to distinguish them from the above mentioned ''condensed'' ones.

In our experiments (100) oriented Si wafers were implanted with He^+ ions at room temperature using energies of 10 and 40 keV and doses of 1×10^{15}, 1×10^{16}, and 5×10^{16} cm^{-2}. After implantation the wafers were furnace annealed at 800 °C for 10 min in nitrogen. Cross sectional transmission electron microscopy (XTEM) and plan view TEM specimens were conventionally prepared and examined on a Philips CM 300 microscope. Elastic recoil detection (ERD) measurements were performed using a primary beam of 35 MeV Cl^{7+} ions as described elsewhere.[6] The depth resolution Δx and the He detection sensitivity were 25 nm and 0.1 at. %, respectively.

For the low dose of 1×10^{15} cm^{-2} (peak He concentration of 4×10^{19} cm^{-3}), no cavities were seen in either the as implanted or annealed samples. This is consistent with previous work,[4,5] where the minimum He concentration required to form He bubbles after annealing was estimated to be 3.5×10^{20} cm^{-3}. At the medium dose of 1×10^{16} cm^{-2} there was no clear evidence for the presence of cavities in the as implanted state. It is worth noting that cavities of a diameter $\Phi<1$ nm cannot be clearly identified in thick TEM samples because of the limited resolution of the kinematic outfocus imaging conditions and/or sample preparation peculiarities. After annealing, however, a diluted system of large cavities was observed. The dimensions and morphology of the cavity arrangements may change with implantation energy. XTEM micrographs from the 10 keV implant revealed that cavities were formed in a well-defined buried layer at a depth of 100 nm. A close inspection over individual sample regions showed that the cavity diameter was in the range $19.5<\Phi<31$ nm with a mean value $\Phi_m\approx26$ nm and standard deviation $\sigma\approx4$ nm. A buried layer of dislocation loops located just below the cavity containing region was also evident.

Figure 1(a) is a plan view micrograph from the 40 keV, 1×10^{16} cm^{-2} implant showing a general appearance of the

[a]On leave from Depto. de Metalurgia–UFRGS, CxP 15051, 91501-970 Porto Alegre, RS, Brazil. Electronic mail: fichtner@if.ufrgs.br

 0003-6951/97/70(6)/732/3/$10.00

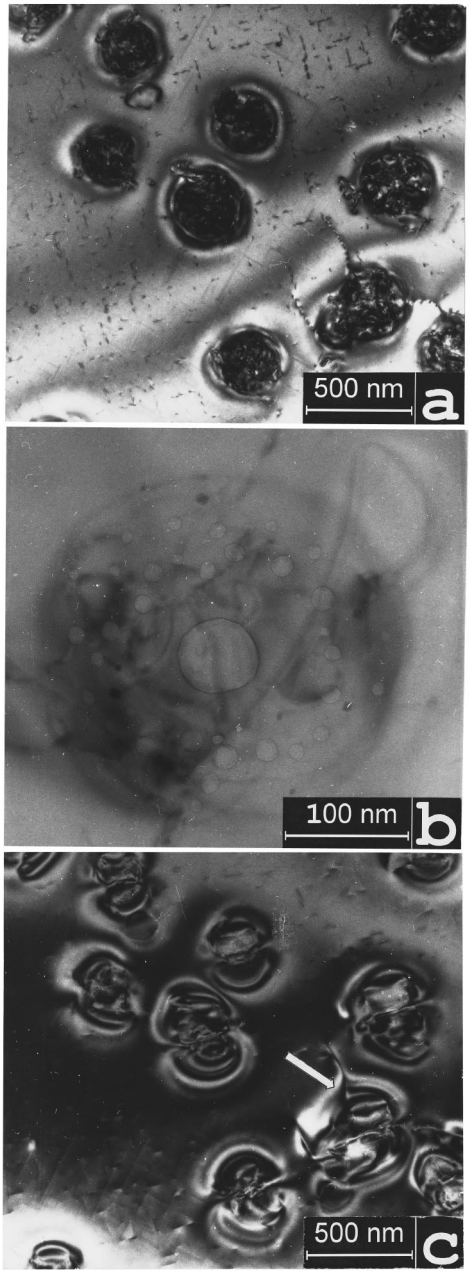

FIG. 1. Plan view TEM micrograph showing a cavity system resulting from the 40 keV, 1×10^{16} cm^{-2} implant after a 10 min, 800 °C anneal. (a) General appearance of the cavities along with dislocation loops. Analysis conditions: dynamic bright field image with electron beam parallel to the ⟨100⟩ axis, multibeam, underfocus. (b) A typical large cavity surrounded by a ring of smaller ones. Analysis conditions: kinematic bright field image, underfocus. (c) A strain field contrast around the cavities and dislocation loops (marked with an arrow) emerging from the strained structure. Analysis conditions: dynamic bright field with electron beam close to the ⟨100⟩ lattice direction, $g=400$, underfocus.

cavity system together with a network of dislocation loops. A typical cavity arrangement observed in an enlarged micrograph from the same implant is shown in Fig. 1(b). The large central cavities are always surrounded by a number of smaller ones forming ''planetary-like'' cavity configurations. It is interesting to note that the small cavities are preferentially distributed in a plane parallel to the sample surface and are arranged within a well defined ''ring'' zone. The diameter of the large central cavities was found to be in the range $27.2<\Phi<75.3$ with $\Phi_m\approx57$ nm and $\sigma\approx9.5$ nm. Figure 1(c) clearly demonstrates the presence of a strong strain field around the planetary-like configurations and dislocation loops running from the cavities. Such features have been previously observed in the case of overpressurized bubbles, i.e., when the gas pressure inside the bubble exceeds the thermodynamic equilibrium condition.[7,8] Furthermore, to our knowledge, neither strain fields nor dislocations can originate from voids or even form equilibrium bubbles (here equilibrium means that the gas pressure inside the bubble is balanced by the surface tension of the matrix). Hence, in light of the above evidence, it is logical to consider that the observed cavities for the 10 and 40 keV implants are not empty but are rather filled with gas, i.e., these are bubbles in an overpressurized state. At the same time, it is important to point out that, within the detection limit of ERD analysis, no He was detected in the annealed sample for the 10 keV implant, and only a small amount of He was measured for the 40 keV implant, which can be attributed to the dilution of the bubbled systems. In fact, from the plan view micrographs of the 40 keV implants, the concentration of planetary-like bubble arrangements was determined to be 2.2×10^{8} cm^{-2}. Thus, assuming that the total He content corresponds to the He sensitivity limit of ERD (5×10^{19} He cm^{-3}), one arrives at an average value of 3.2×10^{6} He atoms per planetary structure. For comparison, the He content inside an equilibrium bubble of a diameter $\Phi\approx57$ nm calculated using the real gas equation of state[9] and a specific surface free energy $\gamma=3$ N m^{-1} for the Si matrix, is 1.5×10^{6}. This means that the average He content in the planetary structures is about a factor of 2 larger than the amount expected for an equilibrium bubble with the same average size as the large ones in the center of the planetary structures. Considering that the He content within the satellite bubbles cannot be large, the combined TEM and ERD results give further support to the concept of overpressurized bubbles discussed above.

For the high dose of 5×10^{16} cm^{-2} the situation is quite different. A dense array of small cavities within the $1.1\leqslant\Phi\leqslant4.5$ nm range is already observed in the as implanted samples. Upon annealing the cavities grow and cluster in a well defined buried layer, consistent with what is known about the He induced structures resulting from similar implants. The mean diameters as well as the maximum and minimum cavity diameters for the 10 keV implant are found to be 7.5, 2.9, and 17.2 nm, respectively. The largest cavity diameter observed in the high dose case appears to be smaller than the smallest one for the medium dose case. This means that each dose used leads to the formation of a substantially different cavity system, and the appropriate differences can be quite well represented by the mean diameter values. In the case of the 40 keV implant Φ was in the range 1.8–18.5 nm and Φ_m was 8.5 nm. Furthermore, for the high dose only a slight increase (from 7.5 to 8.5 nm) in the mean diameter was observed as the implant energy was increased from 10 to 40 keV. Thus, with increasing energy, the differences in cavity size, morphology, and spatial arrangement between the medium and the high dose cases become rather noticeable. It must also be noted that no strain field features associated with individual cavities were observed in condensed cavity systems. This reinforces the inference that

such cavities are not bubbles in an overpressurized state as observed in diluted systems. The He content in the as implanted and annealed samples for the 40 keV implantation was evaluated by ERD and it was found that about 20% of the implanted He was still present within the cavity layer (not shown here). According to the first order gas release model[1] $\ln(N/N_0) = -(3P/rR)\exp(-E_p/kT)t$, where N is the number of He atoms that remain inside the bubbles, N_0 is the initial gas content, t is the time, P is the He permeation rate factor, R is the distance from the bubbles to the sample surface, r is the mean bubble radius, and E_p is the permeability activation energy. It should be pointed out that the constant radius approximation leads to an overestimation of the calculated release time. Nevertheless, using our experimental values $R \approx 350$ nm, $r \approx 4.2$ nm, and $N/N_0 \approx 0.2$, together with the parameters $E_p = 1.7$ and $P = 2.6 \times 10^8$ nm^2 s^{-1} taken from the literature,[4,10] the calculated value of $t = 2.8 \times 10^2$ s is about half of the experimental one. Such a discrepancy arises possibly from an inappropriate use of the parameters E_p and P, which have been obtained under different experimental conditions and within a temperature range 950–1200 °C.[10] Indeed, recent He diffusion studies by Jung[11] have shown that when the He concentration exceeds 5×10^{17} cm^{-3} the He diffusivity is significantly reduced, especially for temperatures below 800 °C, due to He–He interactions. In our case, the maximum He concentration for the 5×10^{16} cm^{-2}, 40 keV implant is 3.5×10^{21} cm^{-3}. Hence, for such high concentrations, it is likely that not only the He–He interactions but also interactions with He–vacancy complexes influence the He permeation. This in turn may explain the discrepancy between the calculated and experimental results.

One can classify the cavity nucleation and growth phenomena in He implanted and annealed Si in terms of three different regimes depending on the implanted He content. The low He concentration regime is characterized by the formation of small He-vacancy (He_mV_n) complexes which may dissociate at rather low temperatures (e.g., $T \approx 250$ °C), as found by Van Veen *et al.*[12] The high He concentration regime can be characterized by the formation of small bubbles already during implantation. With increasing temperature, bubble coarsening takes place simultaneously with the process of He release from bubbles and evaporation from the surface, as proposed by Griffioen *et al.*[1]

For the medium He concentration regime the situation seems to be more complicated. Our experiments do not give clear evidence for the presence of bubbles in the as implanted samples. However, it is reasonable to assume that, if small bubbles are formed either during implantation or at later stages by thermal nucleation, their coarsening evolution should also be influenced by the He release process as in the high concentration regime. Hence, it is difficult to explain the formation of the observed diluted system containing large and overpressurized bubbles in terms of the basic bubble coarsening mechanisms.[9,13] Instead, it seems more rational to consider alternative routes of the microstructure evolution which such medium dose systems may follow. One particular possibility to be further considered is the concept of nucleation and growth of plateletlike, He filled structures.[14] Such ''platelet'' bubbles have previously been observed by Evans *et al.*[8] in He implanted Mo samples. The authors argue that the platelet structures represent a very high He to vacancy ratio and also observe generation of dislocation and strain contrast around the platelets. In addition, they find a transition from the platelet morphology into a group of several spherical bubbles of typical diameters within the 2–3 nm range. In our case, one can assume that some more stable He_mV_n complexes are formed during implantation. Upon annealing these may grow as a platelet bubble up to a given critical size where a transition from a platelet to sphericallike morphology takes place. This morphological change would also imply a transformation from He_mV_n structures containing a large He to vacancy ratio into a real gas phase, which indeed can lead to overpressurized bubble formation. It is also expected that the overpressurized bubble state lasts during a transition period dictated by the finite rate values of the He release process, on the one hand, and by the supply of thermal vacancies, on the other. These two processes should be retarded when the bubble layer is located at larger depths. In this sense, the above concepts are consistent with the experimental evidence for the accumulation of larger overpressure in the case of 40 keV implants as compared with the 10 keV ones.

In summary, we have studied cavity systems formed in Si by implanting He^+ ions at 10 or 40 keV over a dose range $1 \times 10^{15} - 5 \times 10^{16}$ cm^{-2} followed by annealing at 800 °C for 10 min. When the amount of implanted He is sufficiently small or, alternatively, large enough, our results are consistent with those reported by other authors. However, for a critical dose corresponding to a maximum He concentration of 3.5×10^{20} cm^{-3}, one observes a diluted system of large and overpressurized bubbles. The formation of such bubbles cannot be consistently explained in terms of the conventional bubble coarsening mechanisms. Instead, we have proposed an alternative evolution route based on the concept of formation of plateletlike, He filled structures with a subsequent transition into sphericallike morphology.

Two of us (P.F.P.F. and J.R.K.) would like to acknowledge support from Alexander von Humboldt Foundation and CNPq–Brazil, respectively.

[1] C. C. Griffioen, J. H. Evans, P. C. de Jong, and A. van Veen, Nucl. Instrum. Methods Phys. Res. B **27**, 417 (1987).
[2] S. M. Myers, D. M. Bishop, D. M. Follstaedt, H. J. Stein, and W. R. Wampler, Mater. Res. Soc. Symp. Proc. **283**, 549 (1993).
[3] W. Skorupa, N. Hatzopoulos, R. A. Yankov, and A. B. Danilin, Appl. Phys. Lett. **67**, 2992 (1995).
[4] V. Raineri, P. G. Fallica, G. Percolla, A. Battaglia, M. Barbagallo, and S. U. Campisano, J. Appl. Phys. **78**, 3727 (1995).
[5] S. M. Myers and D. M. Follstaedt, J. Appl. Phys. **79**, 1337 (1996).
[6] U. Kreißig, R. Grötzschel, and R. Behrisch, Nucl. Instrum. Methods Phys. Res. B **85**, 71 (1994).
[7] H. Ullmaier, in *Fundamental Aspects of Inert Gases in Solids*, edited by S. E. Donnelly and J. H. Evans (Plenum, New York, 1991), p. 277.
[8] J. H. Evans, A. van Veen, and L. M. Caspers, Radiat. Eff. **78**, 105 (1983).
[9] H. Trinkaus, Radiat. Eff. **78**, 189 (1983).
[10] A. van Wieringen and N. Wartmoltz, Physica **22**, 849 (1956).
[11] P. Jung, Nucl. Instrum. Methods Phys. Res. B **91**, 362 (1994).
[12] A. van Veen, H. Schut, R. A. Hakvoort, A. Fedorov, and K. T. Westerduin, Mater. Res. Soc. Symp. Proc. **373**, 499 (1995).
[13] P. F. P. Fichtner, H. Schroeder, and H. Trinkaus, Acta Metall. Mater. **39**, 1845 (1991).
[14] M. D'Olieslaeger, G. Knuyt, L. De Schepper, and L. M. Stals, in Ref. 10, p. 27.